

GBT Memo 279
MUSTANG-2 Loading and Bandpass Calculations

Brian S. Mason (NRAO)

v1: 08jun12

v2: 25jun12

v3: 29jun12

Abstract

The choice of an optimum bandwidth for broadband continuum measurements involves a trade off between the beating down the photon noise with broader bandwidth, versus degraded telescope efficiency at the higher frequencies and increasing atmospheric loading at the edges of the band, particularly at the lower frequencies. We present a calculation of the optimal bandwidth for a broadband 3mm continuum instrument on the GBT assuming sky-background limited performance and a $240\ \mu\text{m}$ surface. The optimum bandwidth depends on the source spectrum and sky loading, but not strongly so. For efficient broad-band feeds which illuminate the primary aperture the same at all frequencies, very broad bands are favored (~ 72 to 110 GHz). For simpler feeds with beam widths $\propto 1/\nu$, narrower bands are favored (~ 75 to 105 GHz); these feeds incur a penalty of 1.4 in point source sensitivity. A bandwidth of 75 to 105 GHz— close to the current design parameters of the OMT— is reasonably close to the optimum for expected range of source spectra and sky noise levels. We also calculate the total sky loading over each bandpass. For a 75 to 105 GHz square bandpass, 10mm PWV (zenith $\tau \sim 0.12$), 2 airmasses, the current OMT coupling model, and an additional 50% optical efficiency factor, the single-polarization loading from the sky is 13.8 pW. This number does not include cryogenic loading or any safety margin.

Contents

1	Signal to Noise	1
2	Choice of Bandpass	6
3	Variation in Illumination Efficiency across the Band	10
4	Extended Sources	10
5	Loading	11
6	Summary & Conclusions	12
A	Appendix: Rayleigh-Jeans Limit for Radiometer Noise	14

1 Signal to Noise

We seek to compute the signal to noise for a broad, 3mm band receiver on the GBT in the idealized case that the noise is determined purely by the photon statistics of the total loading seen at the receiver input; and to do so for a variety of bandpasses in order to optimize the bandpass choice. Assume the telescope is looking at a uniform sky background with brightness temperature T_{sky} . Approximating the atmosphere as a grey body at temperature T and having optical depth τ , we have $T_{sky} = \epsilon T = T(1 - e^{-\tau})$. At the GB site at 3mm characteristic values at zenith are $T \sim 270$ K, $T_{sky} \sim 27$ K and $\tau \sim 0.1$. In the Rayleigh-Jeans limit— which we do not assume, but which is valid for the atmosphere since $h\nu \ll kT$ — the power per unit bandwidth collected is $P_\nu = kT_{sky}$ independent of frequency. Assume the bandwidth is defined by a bandpass function W . The normalization of this function is arbitrary but for the moment assume it is everywhere ≤ 1 . Consider that we measure the average total power collected P_{tot} in integrations of duration t . The RMS noise in the determination of P_{tot} in each integration can be shown to be

$$\sigma(P_{tot}) = \frac{1}{\sqrt{t}} \sqrt{\int d\nu (h\nu)^2 W n \epsilon (W n \epsilon + 1)} \quad (1)$$

including both “shot-noise” (poisson) and “photon bunching” (Bose/radiometer equation) contributions (Sayers 2008, Richards 1994). The Rayleigh-Jeans, radiometer-equation limit of this equation is considered in the Appendix. Here $n(\nu) = 1/(e^{h\nu/kT} - 1)$ is the photon occupation number for a black body at thermodynamic temperature T ; $W(\nu)$ is the optical efficiency as a function of frequency, i.e., the bandpass function; and $\epsilon(\nu)$ is the emissivity, $(1 - e^{-\tau(\nu)})$ in the case we consider.

We used the ATM code (Pardo et al. 2001) to compute T_{sky} from 60 to 120 GHz for 5mm and 10mm precipitable water vapor (PWV) and the GB site elevation, resulting in the zenith sky brightness temperatures shown in Figure 1. The zenith optical depth is

$$\tau(\nu) = -\ln(1 - T_{sky}(\nu)/T) \quad (2)$$

Assuming an average line of sight physical temperature of 270 K these give optical depths of ~ 0.08 and 0.12 , respectively, which are comparable to the range of good-weather optical depths at the GB site derived by more sophisticated models that include, for example, vertical profile data¹. We use both $T_{sky}(\nu)$ and $\tau(\nu)$ calculated in the manner described above in our bandpass optimization calculation.

We include also the photon noise contributions due to ground spillover— assumed 7K and constant across the band; modeled as a 270K grey body with an emissivity of 0.025— and the CMB— modeled as a 2.7K black body. In this

¹ ‘‘<http://www.gb.nrao.edu/~rmaddale/Weather/index.html>’’

case $n\epsilon$ in Eq. 1 becomes

$$n\epsilon \rightarrow \sum_i n_i \epsilon_i \quad (3)$$

where the sum is over individual grey-body spectra i .

Assuming an unresolved source of flux density S_ν , the source signal collected per unit bandwidth is

$$P_\nu = \frac{1}{2} A_{eff} S_\nu e^{-\tau(\nu)} \quad (4)$$

where $\tau(\nu)$ is the sky optical depth along the line of sight. Then the total source power collected is

$$P_{src} = \frac{1}{2} \int d\nu A_{eff}(\nu) S_\nu W(\nu) e^{-\tau(\nu)} \quad (5)$$

where $A_{eff}(\nu)$ is the telescope effective collecting area as a function of frequency and S_ν is the source flux density as a function of frequency. We have assumed sensitivity to only a single polarization.

The signal-to-noise is then

$$SNR = \frac{P_{src}}{\sigma(P_{tot})} = \frac{\sqrt{t} \int d\nu A_{eff}(\nu) S_\nu W(\nu) e^{-\tau(\nu)}}{2 \sqrt{\int d\nu (h\nu)^2 W n\epsilon (W n\epsilon + 1)}} \quad (6)$$

We parameterize the GBT effective collecting area A_{eff} as

$$A_{eff} = \eta_{illum} \times \eta_{surface} \times A_{geometrical} \quad (7)$$

$\eta_{surface}$ is calculated from the Ruze equation assuming a surface RMS of 240 μm . We assume $\eta_{illum} = 81\%$ independent of frequency (although see § 3). The result is shown in Figure 2.

Some sense of the sensitivity as a function of wavelength can be obtained by considering the quantity $A_{eff}(\nu) S_\nu e^{-\tau(\nu)} / T_{sky}(\nu)$, which is displayed in Figure 3. It is difficult to make quantitative inferences from this plot, however. Since signal adds coherently across the band and noise only incoherently (quadratically), it is necessary to actually carry out the calculation shown in Eq. 6. The net effect of the full calculation compared to what Fig. 3 might suggest is to extend the band on the lower end, where the prevalent effect is increasing (incoherent) noise, and to curtail the band on the high end where the prevalent effect is declining (coherent) signal.

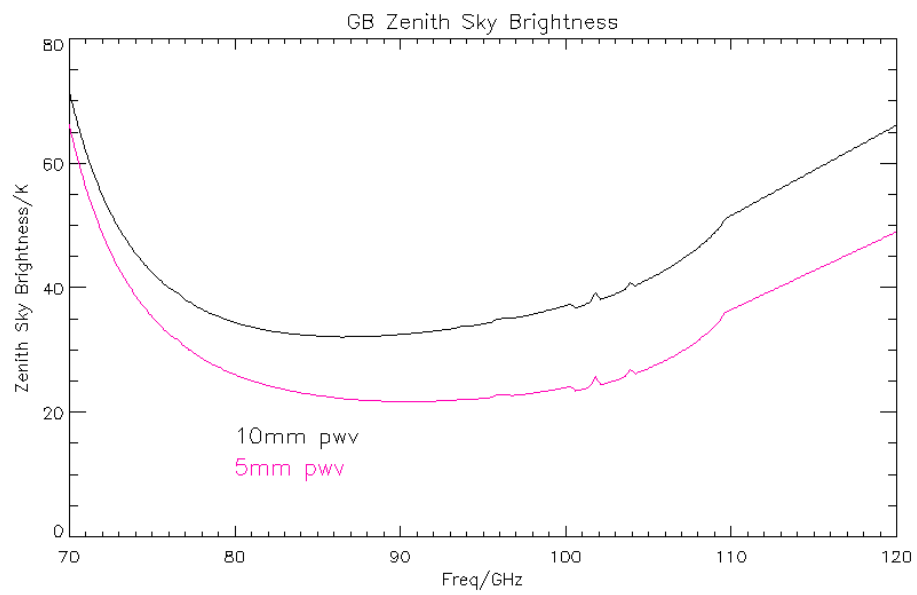


Figure 1: Atmospheric brightness temperature in Green Bank at zenith for 5mm and 10mm precipitable water vapor.

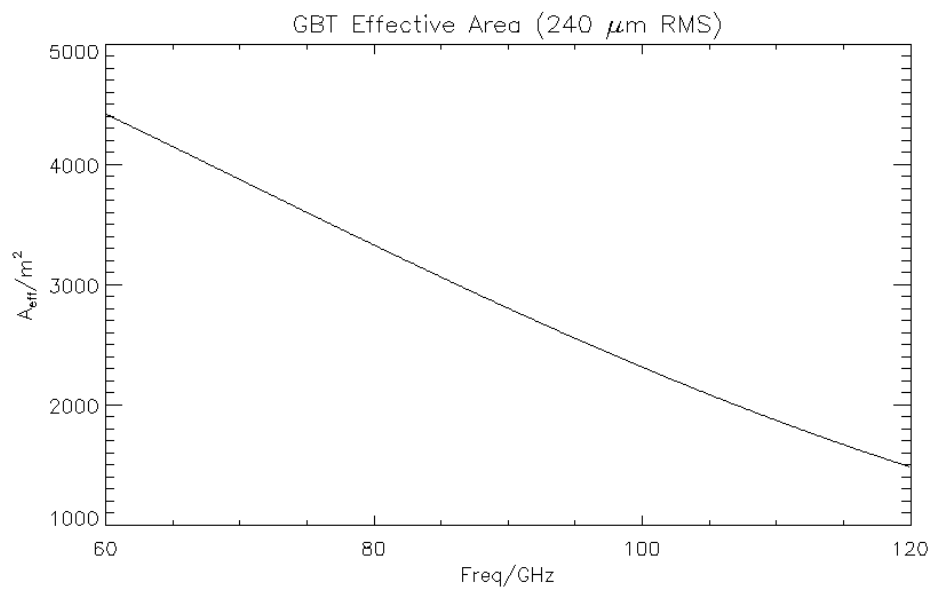


Figure 2: GBT effective collecting area as a function of frequency for a $240\ \mu\text{m}$ ruze-equivalent surface, assuming a constant 81% illumination efficiency.

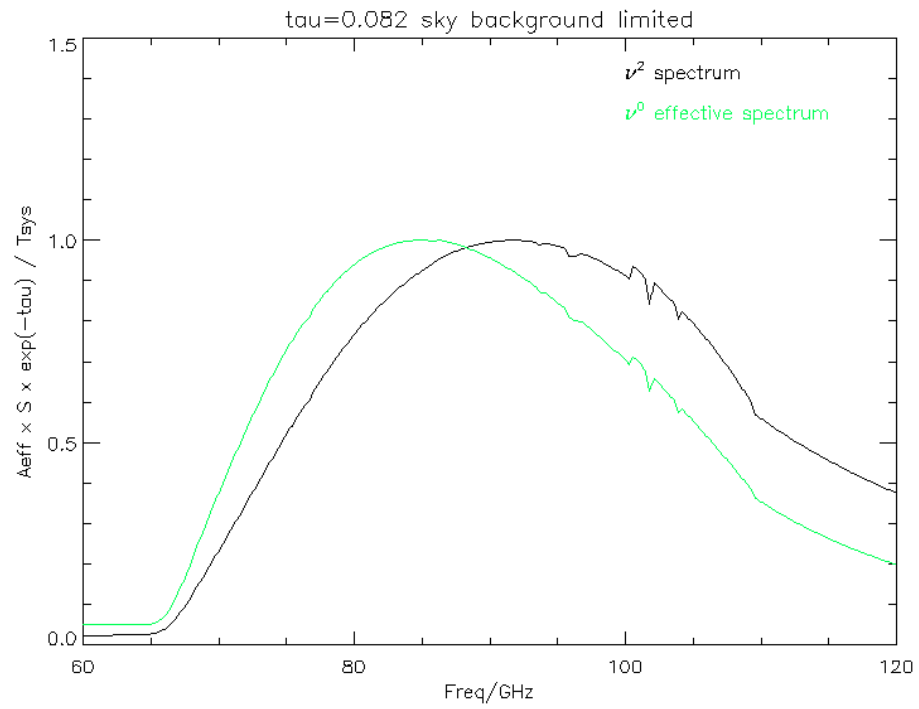


Figure 3: $A_{eff} S_{\nu} e^{-\tau(\nu)} / T_{sky}(\nu)$ for 5mm PWV and a 240 micron surface. Both a flat-spectrum and a thermal spectrum point source are shown. This does not include the calculated OMT coupling efficiency (Fig. 5).

PWV (mm)	Source spectrum	Lower cutoff (GHz)	Upper cutoff (GHz)	SNR
5	ν^0	72.0	108.5	3.61
5	ν^2	74.0	113.0	3.62
10	ν^0	70.5	107.5	2.69
10	ν^2	72.0	114.0	2.64

Table 1: Optimum square bandpass values for constant illumination efficiency.

2 Choice of Bandpass

We have used Eq. 6 to compute the SNR for a grid of rectangular bandpasses characterized by a lower and an upper cutoff. The baseline observing scenario for defining the bandpass assumes: 5mm PWV; 45 degrees elevation (1.4 airmasses); a 1 mJy source at 90 GHz with a flat spectrum; 7K ground spillover, constant across the band; 2.7K of CMB; a 50% optical efficiency, flat across the band; an 81% illumination efficiency, constant across the band; and a 240 μm Ruze-equivalent RMS GBT surface. The upper and lower bandpass cutoffs which maximize the SNR are shown in Table 1 along with the SNR achieved (on a fiducial 1 mJy source in 1 second). This table also presents the results obtained for several other scenarios. A contour plot of the SNR for the full grid of bandpasses is shown for the flat-spectrum, 5mm PWV case in Figure 4.

The TES detectors planned for MUSTANG-2 are coupled to free space via a microstrip OMT. The coupling efficiency of this OMT as currently designed is shown in Figure 5. The dashed magenta contours in Figure 4 show what happens when this coupling efficiency is included. The main effect is to weaken the constraint on the lower end of the band since the OMT is cutting off the band there.

Identical calculations were carried out for 10mm PWV and 30 degrees elevation, with results shown in Figure 6. The effect of this is to reduce the SNR and favor extending the lower end of the band toward 70 GHz.

This analysis optimizes for *point source sensitivity*. Extended sources are considered in § 4.

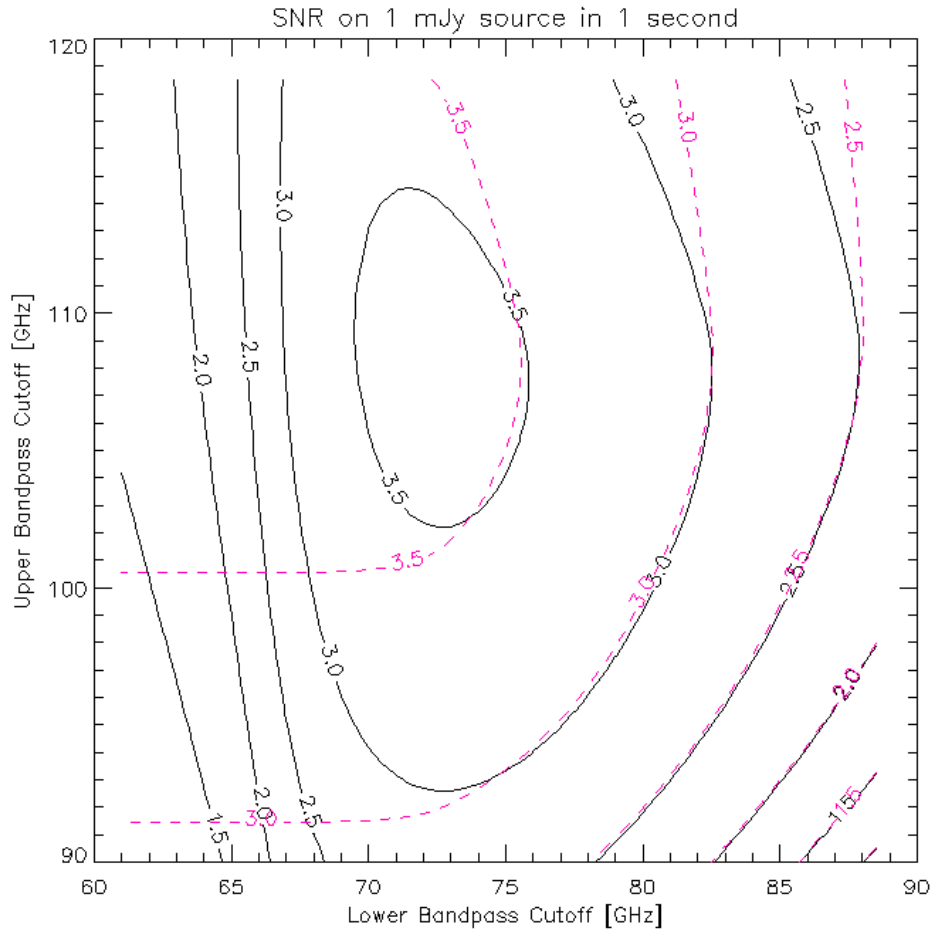


Figure 4: SNR (levels 1, 1.5, 2, 2.5, 3, 3.5) in 1 second as a function of upper and lower bandpass cutoffs for 5mm PWV, 45 degrees elevation, flat spectrum 1 mJy (at 90 GHz) point source. Magenta dashed lines (same contour levels) show the result of including the calculated MUSTANG-2 OMT coupling efficiency.

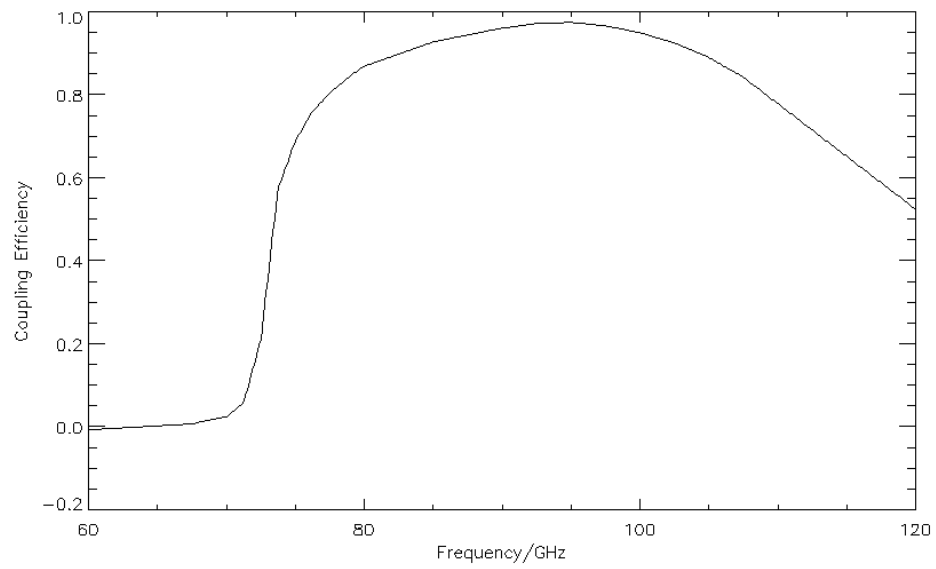


Figure 5: Calculated MUSTANG2 OMT coupling efficiency vs frequency (from Jeff McMahon, 03jan12 model run).

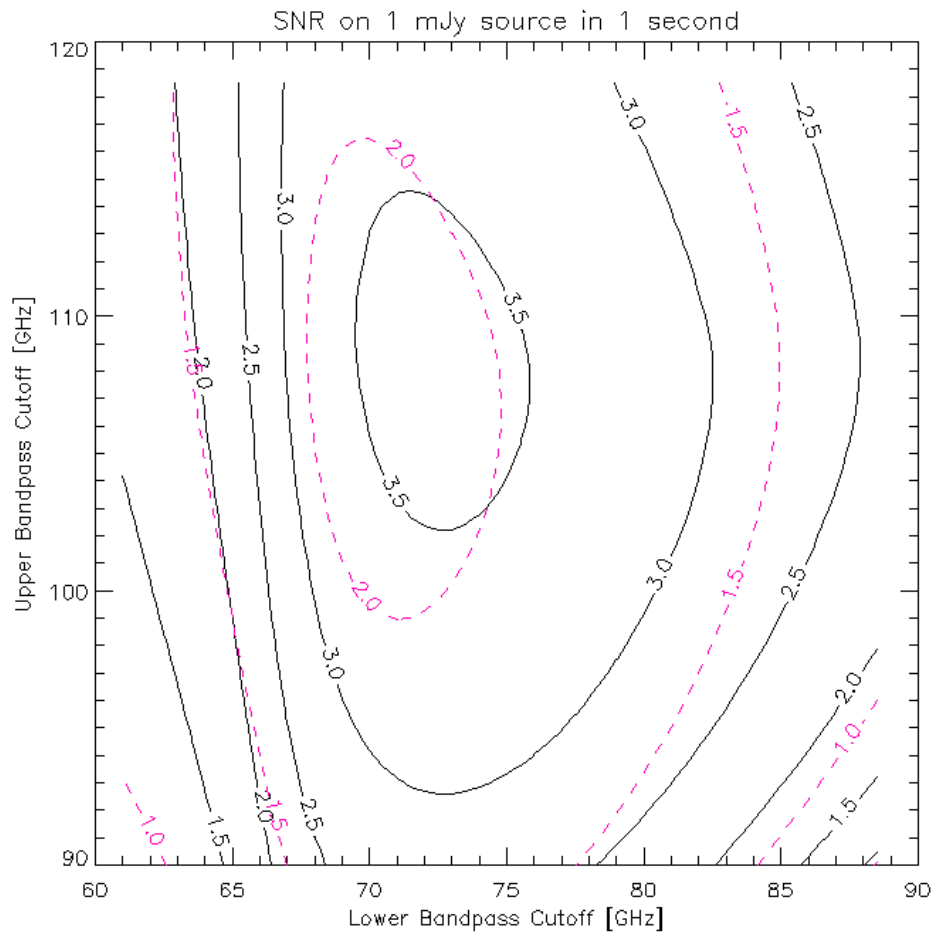


Figure 6: Same as Fig. 4, but here the dashed magenta contours show the SNR contours assuming 10mm PWV and 30 degrees elevation.

PWV (mm)	Source spectrum	η_{illum}	Lower cutoff (GHz)	Upper cutoff (GHz)	SNR
5	ν^0	const.	72.0	108.5	3.61
5	ν^0	$\propto \nu^{-2}$	75.0	103.0	2.59
5	ν^2	const.	74.0	113.0	3.62
5	ν^2	$\propto \nu^{-2}$	80.0	107.5	2.54

Table 2: Optimum square bandpass values, constant vs. varying illumination efficiency.

3 Variation in Illumination Efficiency across the Band

Many of the simple-to-machine, array-feedhorn designs being considered result in beams which decrease in width with increasing frequency as

$$\text{FWHM}_{\text{feedhorn beam}} \sim 1/\nu. \quad (8)$$

Feeds optimized for good broad-band performance, in contrast, provide more nearly constant feedhorn beams with varying frequency, increasing the point source sensitivity. The SNR achieved on a resolved source is to first order not affected since the larger beam will collect more flux, approximately counteracting the smaller effective area.

To quantify this we have examined a fiducial limiting case where the illumination efficiency

$$\eta_{illum} = 81\% \times \left(\frac{\nu_{min}}{\nu}\right)^2 \quad (9)$$

where ν_{min} is the lower cutoff of the square bandpass. This seems to describe the performance expected of current, preliminary feedhorn designs, although more detailed investigation is needed. The results are shown in Table 2. There is a factor of ~ 1.4 loss in point source gain for the bandwidths under consideration.

4 Extended Sources

The calculations carried out in the previous sections assume *unresolved* sources. We will consider two cases of resolved source observations: i) constant A_{eff} vs frequency but $\Omega_{main\ beam} \sim 1/\nu^2$ (broad-band feed); ii) $A_{eff} \sim 1/\nu^2$ (due to decreasing illumination efficiency with increasing frequency) but $\Omega_{main\ beam}$ constant. We will show that the SNR for resolved source observations is the identical in these two cases, and equal to that obtained by a broad-band feed observing an *unresolved* source with a different spectrum.

For the broad-band feed case (i), assume $A_{eff} = A_o$, $\Omega_{mb} = \Omega_{mb,o} \times \left(\frac{\nu_o}{\nu}\right)^2$, and that the unresolved source observed has a surface brightness $I_o \times \left(\frac{\nu}{\nu_o}\right)^\alpha$.

Then the spectral power collected is

$$P_\nu = A_o I_o \times \left(\frac{\nu}{\nu_o}\right)^\alpha \Omega_{mb,o} \times \left(\frac{\nu_o}{\nu}\right)^2 \quad (10)$$

This is the same spectral power as would be seen observing an *unresolved* source with flux density $S_\nu = I_o \times \left(\frac{\nu}{\nu_o}\right)^{\alpha-2} \Omega_{mb,o}$.

For the other case (ii), assume $A_{eff} = A_o \times \left(\frac{\nu_o}{\nu}\right)^2$, $\Omega_{mb} = \Omega_{mb,o}$, and that the unresolved source observed has a surface brightness $I_o \times \left(\frac{\nu}{\nu_o}\right)^\alpha$. Then the spectral power collected is

$$P_\nu = A_o \times \left(\frac{\nu_o}{\nu}\right)^2 I_o \times \left(\frac{\nu}{\nu_o}\right)^\alpha \Omega_{mb,o} \quad (11)$$

This is also the same spectral power as would be seen *using the feed in case (i)* observing an unresolved source with flux density $S_\nu = I_o \times \left(\frac{\nu}{\nu_o}\right)^{\alpha-2} \Omega_{mb,o}$.

High-resolution SZE observations are one important science driver for this instrument. These can be considered to be approximately unresolved observations of a thermal-spectrum source. From the point of view of the optimization analysis this is equivalent to observing an unresolved flat-spectrum target with an efficient broad-band feed, with the resulting SNR being independent to first order on how the feed illumination varies with frequency.

5 Loading

The specific intensity (spectral surface brightness) of a grey body is

$$I_\nu = 2 \frac{h\nu}{\lambda^2} \frac{\epsilon}{e^{h\nu/kT} - 1} \quad (12)$$

including contributions from both polarizations. The spectral power collected in a single polarization by an antenna with collecting area A_{eff} looking into this (uniform, completely beam-filling) black body is

$$P_\nu = \frac{A_{eff}}{2} \int d\Omega I_\nu = \frac{A_{eff}}{2} \Omega_{ant} I_\nu = \epsilon \frac{h\nu}{e^{h\nu/kT} - 1} \quad (13)$$

Assume we measure total power collected over a band pass $W(\nu)$, the value of which represents the total optical efficiency of the system at a given frequency. Then we have

$$P_{tot} = \int d\nu \frac{h\nu}{e^{h\nu/kT} - 1} \epsilon(\nu) W(\nu) \quad (14)$$

We assume 10mm PWV and $A = 2$, i.e., observations at 30° elevation; an overall $\eta_{opt} = 50\%$; and the ground and CMB contributions previously described. This amounts to an equivalent $T_{sys} \sim 74$ K, which would also conveniently allow laboratory characterization using liquid nitrogen.

The resulting sky loadings are shown in Figure 7. For a 75 to 105 GHz bandpass, including the OMT coupling efficiency, ground, and CMB, the resulting single-polarization loading from sky+ground is 13.8 pW. This does not include cryogenic loading, loading from the telescope, or any safety factor.

6 Summary & Conclusions

- The optimization analysis we have done indicates that very broad (~ 40 GHz) bandpasses covering the range from 72 to 110 GHz are favored.
- The SNR is a fairly weak function of the precise band choice with lower band limits between 70 and 77 GHz and upper limits between 100 and 110 GHz. The SNR falls off steeply below 70 GHz.
- Illumination patterns which keep the illumination efficiency constant with frequency across the band deliver $\sim 1.4\times$ higher point source sensitivity compared to a fiducial case where $\eta_{illum} \propto 1/\nu^2$. Resolved-source sensitivity does not depend strongly on how the aperture is illuminated as a function of frequency. Illumination efficiencies which fall across the band tend to favor smaller bandpasses (~ 30 GHz).
- Practically speaking the telescope gain will be more unstable at the upper end (> 100 GHz), favoring the lower end of the band. Calibrating very broad bands will also be more model-dependent.
- For scenario with a 75 to 105 GHz bandpass, 50% optical efficiency times the OMT coupling, 10mm PWV, 2 airmasses, 7K ground spillover, and the CMB total the total loading on a single-polarization detector is 13.8 pW. This does not include cryogenic or telescope loading or a safety factor.

Detailed analysis of specific feedhorn designs will be considered separately in the future.

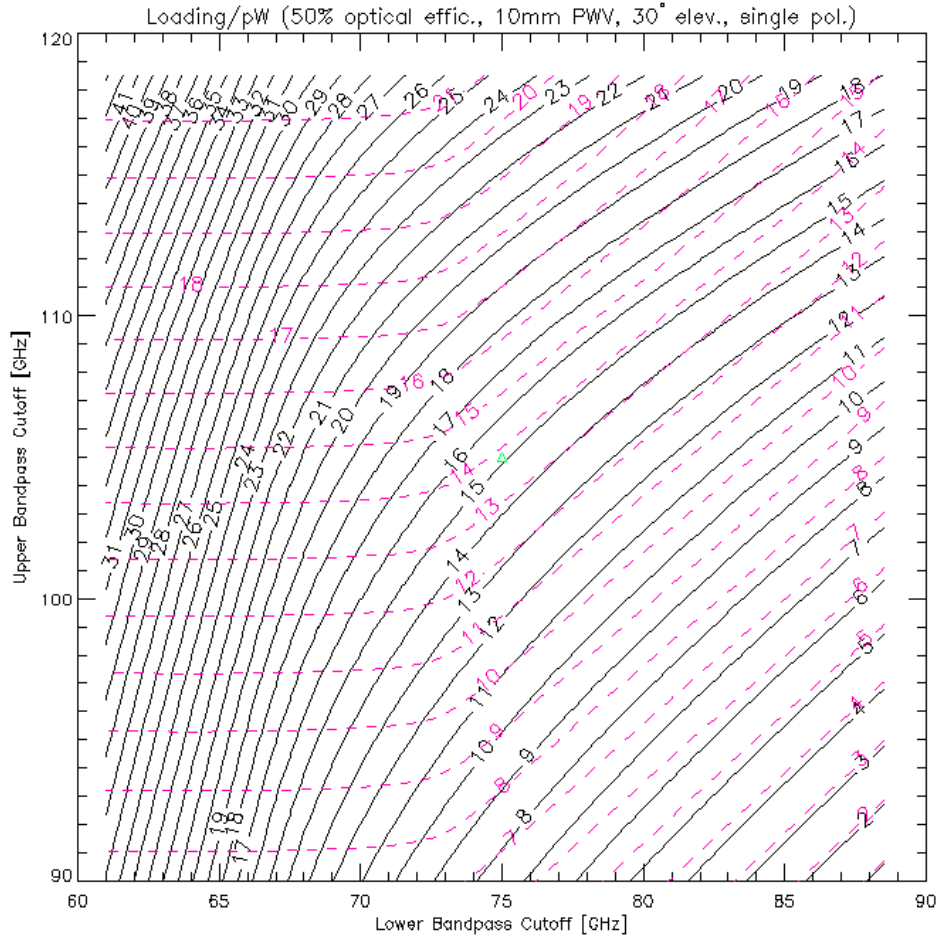


Figure 7: Detector loading from the sky in picoWatts for a grid of bandpasses. All assume $\eta_{opt} = 50\%$; magenta dashed lines show the effect of also including the OMT coupling in Figure 5. We have assumed 10mm PWV and a line of sight at 30 degrees above the horizon. The green triangle is located at (75 GHz, 105 GHz).

A Appendix: Rayleigh-Jeans Limit for Radiometer Noise

In the Rayleigh-Jeans limit, equation 1 for the RMS noise in integrations of length t reduces to

$$\sigma(P_{tot}) = \frac{k}{\sqrt{t}} \sqrt{\int d\nu W^2 T_{sky}^2} \quad (15)$$

This may also be derived from the radiometer equation by considering a case where the T_{sky} is constant in small bins of some width $\delta\nu$. This approximation underestimates the true noise by $\sim 8\%$ in the middle of the band (90 GHz).

The signal-to-noise is then

$$SNR = \frac{P_{src}}{\sigma(P_{tot})} = \frac{\sqrt{t} \int d\nu A_{eff}(\nu) S_\nu W(\nu) e^{-\tau(\nu)}}{2k \sqrt{\int d\nu W^2 T_{sky}^2}} \quad (16)$$

For the case that all quantities inside the integrals are constant over a square bandpass of width $\Delta\nu$, this reduces to the standard result:

$$SNR = \frac{A_{eff} S_\nu e^{-\tau} \sqrt{\Delta\nu t}}{2k T_{sky}} \quad (17)$$

References

- Pardo, J.R., Cernichardo, J. and Serabyn, E. 2001, IEEE Trans. Ant. & Prop. 49, 1683
 Richards, P.L. 1994, J.Apl.Phys. 76, 1
 Sayers, J. 2008, Ph.D. thesis, California Institute of Technology